Check for updates

View Article Online
View Journal

Journal of
Materials Chemistry B

Accepted Manuscript

This article can be cited before page numbers have been issued, to do this please use: Z. Zeng, Z. Wei, L. Ma, Y. Xu, Z. Xing, H. Niu, H. Wang and W. Huang, *J. Mater. Chem. B*, 2017, DOI: 10.1039/C7TB01288H.

This is an Accepted Manuscript, which has been through the Royal Society of Chemistry peer review process and has been accepted for publication.

Accepted Manuscripts are published online shortly after acceptance, before technical editing, formatting and proof reading. Using this free service, authors can make their results available to the community, in citable form, before we publish the edited article. We will replace this Accepted Manuscript with the edited and formatted Advance Article as soon as it is available.

You can find more information about Accepted Manuscripts in the author guidelines.

Please note that technical editing may introduce minor changes to the text and/or graphics, which may alter content. The journal's standard Terms & Conditions and the ethical guidelines, outlined in our author and reviewer resource centre, still apply. In no event shall the Royal Society of Chemistry be held responsible for any errors or omissions in this Accepted Manuscript or any consequences arising from the use of any information it contains.

ROYAL SOCIETY OF CHEMISTRY

rsc.li/materials-b

View Article Online
DOI: 10.1039/C7TB01288H

Journal Name

ARTICLE

pH-responsive nanoparticle based on Ibuprofen prodrug as drug carrier for inhibition of primary tumor growth and metastasis

Received 00th January 20xx,
Accepted 00th January 20xx

DOI: 10.1039/x0xx00000x

www.rsc.org/

Zhi Zeng,[a] Zeliang Wei,[b] Limei Ma,[a] Yao Xu,[a] Zhihua Xing,[a] Hai Niu,[bc] Haibo Wang,*[d] and Wen Huang*[ab]

Cancer metastases represent a major determinant of mortality in patients with cancer. Cyclooxygenase-2 (COX-2) and its metabolites play important roles in tumor growth and metastasis. Overexpression of COX-2 have been found in many types of cancers including melanoma. Nonsteroidal anti-inflammatory drugs (NSAIDs) have been widely used to inhibit COX-2, which could be a promising addictive to the management of aggressive cancers. A novel pH-sensitive drug delivery carrier based on PEG-derivatized ibuprofen— MPEG-PHEI was synthesized to dual-deliver anticancer agents and NSAIDs. This amphiphilic and biodegradable copolymer could self-assemble into core–shell nanoparticles (NPs) and payload hydrophobic doxorubicin (DOX). DOX-loaded MPEG-PHEI nanoparticles (DOX/NPs) could release DOX in endosome microclimate via micelle collapse and ibuprofen via ester bond hydrolysis. *In vitro* DOX/NPs showed comparable cytotoxicity to DOX·HCl, and comparable inhibition of COX-2 to ibuprofen. More importantly, DOX/NPs revealed a significant *in vivo* therapeutic efficacy in both experimental subcutaneous tumors and lung metastasis model, while decreasing the toxicity of DOX. This study demonstrated the advantages of combining NSAIDs with chemotherapy agents, and provided a novel nanoparticle system for both primary and metastatic tumor treatment.

Introduction

Nowadays, cancer is one of the leading causes of morbidity and mortality in the world. In clinics, chemotherapy is highly significant in the treatment of solid tumors, but this approach is usually effective at early stage. Once the tumor has metastases, chemotherapy is much less successful.[1, 2] Clinical researches have revealed that metastases accounts for more than 90% death in cancer patients.[3, 4] Furthermore, metastases are highly resistant to conventional chemotherapies, mainly due to its biological heterogeneity, as well as the effects of organ environment on biological behavior of metastatic cells.[2, 5-7] There is a crucial need to provide new treatment strategies for inhibiting primary tumor and its metastasis at the time of chemotherapy.

The metastatic process is intricate and tightly associated with enzymes, pro-inflammatory cytokines and growth factors, including interleukin (IL), matrix metalloproteinases (MMPs), nuclear factor κB (NF-κB), and cyclooxygenase-2 (COX-2).[8-10] COX-2 overexpresses in many types of cancers such as prostate, colon cancer and melanoma.[11, 12] Cyclooxygenases (COXs) catalyze the rate-limiting step in the formation of prostaglandins (PGs) from arachidonic acid (AA). COX-2 is the inducible isoform of the COX enzyme family. Unlike Cyclooxygenase-1 (COX-1), which plays a key role in maintaining homeostasis, COX-2 plays a key role in inflammation, by inducing stimulate pro-inflammatory cytokines and growth factors.[13, 14] More importantly, COX-2 and its products, especially Prostaglandin E_2 (PGE_2), were found to favor tumor growth and metastasis, which has made COX-2 an important drug target for cancer treatment.[15, 16] Nonsteroidal anti-inflammatory drugs (NSAIDs) such as ibuprofen and aspirin have been widely used to inhibit COX-2. Therefore, a combination of NSAIDs and anticancer drug can be a promising strategy for both primary and metastatic tumors. To date, NSAIDs have been documented to decrease migration.[17] Using adjuvant NSAIDs, including aspirin, naproxen, buprofen, celecoxib and piroxicam, has also been found to decrease the incidence of primary and recurrent cancers including prostate, colon, breast cancer and melanoma, thereby decrease mortality.[18-21]

Over recent decades, polymeric drug delivery systems have been developed as carriers for chemotherapeutic agents to improve drug residence time in tumors, and therapeutic effect, via enhanced permeation and retention (EPR) effect.[22, 23] Numerous investigations have demonstrated that this drug delivery systems could enhance the solubility and

[a] Laboratory of Ethnopharmacology, Regenerative Medicine Research Center, West China Hospita, West China Medical School, Sichuan University, Chengdu 610041, China. E-mail: huangwen@scu.edu.cn
[b] Institute for Nanobiomedical Technology and Membrane Biology, Sichuan University, Chengdu 610041, China. E-mail: niuhai@scu.edu.cn; Fax: +86-028-85164075; Tel: +86-028-85164073
[c] College of Mathematics, Sichuan University, Chengdu, 610045, China
[d] Textile Institute, College of Light Industry, Textile and Food Engineering, Sichuan University, Chengdu, 610065, China. E-mail: wanghaiboo@126.com
*The first corresponding author is W. Huang, E-mail: huangwen@scu.edu.cn and the second is H. Wang, E-mail: wanghaiboo@126.com
Electronic Supplementary Information (ESI) available: [details of any supplementary information available should be included here]. See DOI: 10.1039/x0xx00000x

Published on 25 July 2017. Downloaded by University of Windsor on 25/07/2017 13:36:54.

Journal of Materials Chemistry B Accepted Manuscript

Please do not adjust margins

View Article Online
DOI: 10.1039/C7TB01288H

Published on 25 July 2017. Downloaded by University of Windsor on 25/07/2017 13:36:54.

bioavailability of drugs, thus, allowing them to reach their target sites and reduce side effects.[24, 25] Recently, stimuli-responsive polymeric systems attract much attention. The payload could be released rapidly in response to external trigger such as pH, temperature, or redox potential.[26-29] Among them, pH-responsive drug delivery systems have been widely applied in cancer therapy due to the presence of a remarkable pH gradients between intracellular endosome microclimate (~5.0) and normal tissues (7.4).[30-32] The pH-responsive drug delivery systems were able to keep stable in the blood circulation and release drug rapidly after internalized by cancer cells.[33, 34]

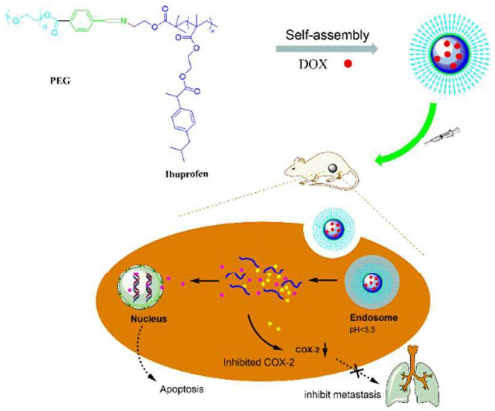

Scheme 1 Schematic illustration: drug loading process of MPEG-PHEI nanoparticles in aqueous solution and pH triggered drug release.

An innovative pH-sensitive, amphiphilic and biodegradable copolymer methoxy poly (ethylene glycol) – b – poly (2-([2-4-(2-methylpropil) phenyl] propionyl] oxy) ethyl methacrylate) (MPEG-PHEI) was synthesized through atom transfer radical polymerization (ATRP). Because of its amphiphilicity, MPEG-PHEI could self-assemble and payload hydrophobic drug in water. Based on previous studies, ibuprofen could be released via ester bond hydrolysis at physiological conditions (37 °C, pH 7.4), and retain its activity.[35, 36] Non-toxic and biocompatible methoxy poly (ethylene glycol) (PEG) was employed as protective shell.[37, 38] DOX-loaded MPEG-PHEI nanoparticles (DOX/NPs) possessed excellent biophysical properties including size, loading capacity, *in vitro* drug release kinetics and biocompatibility. Subcutaneous B16 melanoma tumor model and lung metastasis model were employed to invest *in vivo* anti-tumor behaviours of DOX/NPs. Among all deadly types of cancer, melanoma is particularly deadly because of its propensity to metastasize. Its incidence keeps rising.[39] The overexpression of COX-2 has been frequently observed in both human melanoma specimens and murine models, as in many other types of cancer.[40-42] Our results revealed that DOX/NPs could inhibit the activity of COX-2 *in vivo*, thusly inhibit tumor metastasis.

Experimental

Reagents.

Ibuprofen, 2-hydroxyethyl methacrylate (HEMA), 4-dimethylaminopyridine (DMAP), CuCl, N,N,N',N',N''-Pentamethyldiethylenetriamine (PMDETA), pyrene, ethanolamine, and 2-bromo-2-methylpropionyl bromide were purchased from Aladdin Chemical Co., Ltd. (Shanghai, China). Methanol, tetrahydrofuran (THF), dichloromethane (DCM), petroleum ether (PE), ethyl acetate (EA), ethyl ether, isopropanol, acetone, and N,N′-dicyclohexylcarbodiimide (DCC) were purchased form Chengdu Kelong Chemical Co., Ltd. (Chengdu, China). 4-Formylbenzoic acid (p-CBA) and 1-[3-(dimethylamino)propyl]-3-ethylcarbodiimide methiodide (EDC) were purchased from Energy-chemical (Shanghai, China). Doxorubicin hydrochloride (DOX·HCl) was purchased from Tecoland Corporation (Irvine, CA, USA.). Triethylamine (TEA), 3-(4, 5-dimethylthiazol-2-yl)-2, 5-diphenyl tetrazolium bromide (MTT) and dimethyl sulfoxide (DMSO) were purchased from Sigma-Aldrich (St. Louis, MO, USA). All of the reagents were used as received. PEG (Mn = 2000 g/mol) was purchased from Fluka and dried by azeotropic distillation in the presence of dry toluene.

Dulbecco's modified Eagle's medium (DMEM) was purchased from HyClone, GE Healthcare Life Science (Logan, UT, USA). Fetal bovine serum (FBS) was purchased from Gibco Life Technologies (Carlsbad, CA, USA). Hoechst 33258 was purchased from Biyuntian Biotechnology Co. (Shanghai, China). Mouse monoclonal anti-GAPDH (1:5,000; G8795) were purchased from Sigma-Aldrich (St. Louis, MO, USA). Rabbit monoclonal anti-COX-2 (1:1,000; ab62331) were purchased from Abcam (Burlingame, CA, USA). Cleaved Caspase-3 (Asp175) Rabbit mAb (1:1000; 9664S) were purchased from Cell Signaling Technology Inc (Beverly, MA, USA). Horseradish peroxide-conjugated goat anti-mouse immunoglobulin IgG (1:5,000; sc-2005) and goat anti-rabbit IgG (1:5,000; sc-2004) were purchased from Santa Cruz Biotechnology Inc. (Santa Cruz, CA, USA).

Characterization.

^{1}H-NMR experiments were conducted on an INOVA-400 spectrometer (400 MHz, Varian, USA), using tetramethylsilane (TMS) as internal reference, and $CDCl_3$ as solvent. Gel permeation chromatography (GPC) was performed with Waters-1515 (USA) using N, N-dimethylformamide (DMF)/LiBr as eluent. The molecular weights are relative to narrow polystyrene standards. The flow rate was 1.0 mL/min at 40 °C. The number-averaged W_n and molecular weight distributions (PDIs) of the polymers were measured on a Waters 1515 GPC instrument with a Waters 1515 isocratic HPLC pump, a Waters 2414 refractive index detector, a Waters 717 plus autosampler and a set of MZ-Gel SD plus columns (300 × 8.0 mm, 500 °A, 103 °A and 104 °A). TEM was recorded on a JEOL JEM-100CX-II instrument at a voltage of 200 kV. A drop of nanoparticle solution was placed on a carbon-coated copper grid, and then the liquid was freeze dried in vacuum before measurement. Sizes of nanoparticles were measured on a HORIBA DLS particle size analyzer LB-550 at room temperature. The fluorescence and UV-Vis spectra were determined by F-7000 fluorescence spectrometer (HITACHI, Tokyo, Japan) and DU 800 UV-Vis spectrometer (Beckman Coulter, CA, USA), respectively.

Journal of Materials Chemistry B Accepted Manuscript

This journal is © The Royal Society of Chemistry 20xx

Please do not adjust margins

View Article Online
DOI: 10.1039/C7TB01288H

Published on 25 July 2017. Downloaded by University of Windsor on 25/07/2017 13:36:54.

Synthesis of 2-([2-4-(2-methylpropil)phenyl]propionyl]oxy) ethyl methacrylate (HEI). Ibuprofen (2.1 g) and EDC (2.0 g) was dissolved in 50 mL of DCM in a single neck round flask. HEMA (1.3 g) and DMAP (0.5 g) was added. The mixture was stirred at room temperature for 24 h. Then the solvent was evaporated under vacuum and product was purified by silica gel column chromatograph (EP: EA=15:1, v/v). Yield: 83%. ^{1}H NMR (400 MHz, $CDCl_3$) δ 7.18 (d, 2H, Ar-H), 7.07 (d, 2H, Ar-H), 6.03 (s, 1H, C=CH), 5.54 (s, 1H, C=CH), 4.31 (m, 4H, $COO-CH_2-CH_2$), 3.72 (q, 1H, CH), 2.43 (d, 2H, Ar-CH_2), 1.89 (s, 3H, CH_3), 1.83 (m, 1H, CH), 1.49 (d, 3H, CH_3), 0.89 (d, 6H, CH_3).

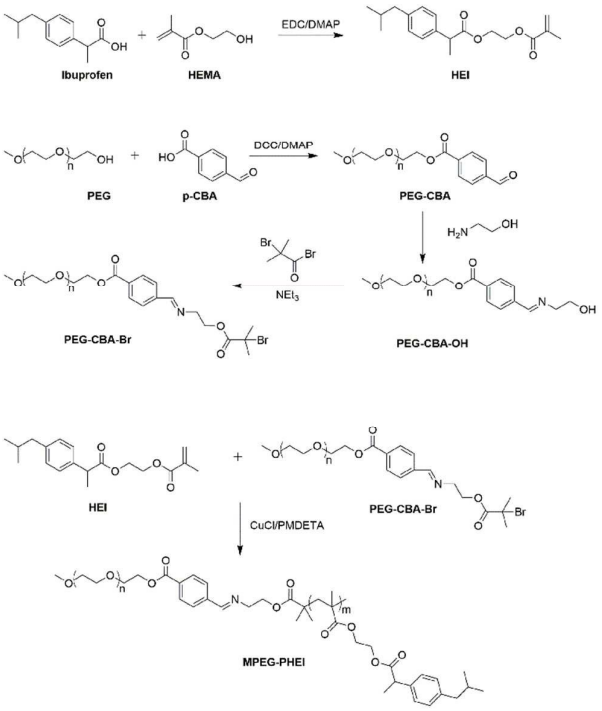

Scheme 2 Synthesis route of precursors and MPEG-PHEI.

Synthesis of PEG-CBA. PEG-CBA was synthesized as the procedure outlined by Song.[43] In briefly, CBA (15.2 g) and PEG (12.6 g) was dissolved in 200 mL DCM. Then DCC (16.5 g) and DMAP (2.4 g) was added into the solution. The reaction solution was stirred gently at room temperature for 60 h. Side product, dicyclohexylurea, was removed by filtration. The solvent was removed by rotational evaporation. The crude product was purified by recrystallization in isopropanol, and in vacuum for 2 days. Yield: 85%. ^{1}H NMR (400 MHz, $CDCl_3$) δ 10.11 (s, 1H, Ar-CHO), 8.25 – 8.20 (d, 2H, Ar-H), 7.99 – 7.94 (d, 2H, Ar-H), 4.55 – 4.49 (t, 2H, CH_2), 3.65 (m, -CH_2- of PEG), 3.38 (s, 3H, -O-CH_3).

Synthesis of PEG-CBA-OH. Ethanolamine (1.8 g) and PEG-CBA (6.5 g) was dissolved in 100 mL of THF, and reaction solution was stirred at 40 °C overnight. The solvent was removed under reduced pressure. The crude product was dissolved in methanol, precipitated in ethyl ether to remove impurities, and further purified by recrystallization in isopropanol. The pure PEG-CBA-OH was dried in vacuum for 2 days. Yield: 90%.

Synthesis of PEG-CBA-Br. PEG-CBA-OH (4.4 g) and TEA (0.6 mL) was dissolved in 50 mL of DCM, and 2-bromo-2-methylpropionyl bromide (0.5 g) was added drop wise into the solution at 0 °C in 20 min. The solution was stirred for 4 h at 0 °C and for another 48 h at room temperature. Side product was removed by filtration. The solvent was removed under vacuum. The crude product was precipitated in ethyl ether to remove impurities, and then in vacuum for 2 days. Yield: 82%. ^{1}H NMR (400 MHz, $CDCl_3$) δ 8.40 (s, 1H, -CH=N-), 8.17 – 8.12 (d, 2H, Ar-H), 7.84 – 7.79 (d, 2H, Ar-H), 4.50 – 4.45 (t, 2H, CH_2), 4.01-3.96 (m, 2H, -CH_2-O-), 3.86-3.79 (m, 2H, -CN-CH_2-), 3.65 (m, -CH_2- of PEG), 3.38 (s, 3H, -O-CH_3), 1.82 (s, 6H, CH_3).

Synthesis of MPEG-PHEI. IBUMA (3.0 g) and PEG-CBA-Br (2.0 g) was dissolved into THF in a three neck round flask. And CuCl (0.02 g) and PMDETA (0.07 g) was added under nitrogen. The reaction was stirred at 50 °C for 24 h under a nitrogen atmosphere. Reaction mixture was separated by on a neutral alumina column (THF), and the solvent was evaporated under reduced pressure to give crude product. The crude product was further purified by methanol precipitation, and dried in vacuum for 2 days. Yield: 59%. ^{1}H NMR (400 MHz, $CDCl_3$) δ 7.36 (d, 4H, Ar-H), 7.18 – 6.95 (d, 81H, Ar-H), 4.31 – 4.10 (s, 86H, -$COO-CH_2$), 3.65 (m, -CH2- of PEG), 3.38 (s, 3H, -O-CH_3), 2.41 (d, 41H, Ar-CH_2-), 2.38 – 1.60 (m, 65H, -C-CH_2), 1.60 – 1.34 (m, 69H, CH_3), 1.25 (s, 6H, CH_3), 0.87 (d, J = 5.5 Hz, 195H, CH_3).

Critical micelle concentration (CMC) measurement.
According to previous study, the CMC was determined by using pyrene as a fluorescence probe.[44] In detail, a predetermined amount of pyrene solution in acetone was added in a series of 4 mL centrifuge tubes, and acetone was evaporated overnight completely. The micelle solution in Milli-Q water in various concentrations were added into each of those pyrene centrifuge tubes, ensure the final concentrations ranged from 5.0×10^{-6} to 0.1 g/L, and pyrene's concentration was 0.12 mg/L. Placed all of the solutions in darkness at room temperature for 2 h to equilibrate pyrene partition between water and micelles. For fluorescence-excitation spectra, the emission wavelength was set to 390 nm and the excitation bandwidth was 5.0 nm. The scan speed was 240 nm/min.

Nanoparticle formation.
10 mg MPEG-PHEI was dissolved in 1 mL DMSO. 100 μL of this solution was added into 400 μL of Milli-Q water in drop wise. The mixture was stirred at room temperature for 2 hours, and dialyzed by a dialysis bag (MWCO: 3500) against Milli-Q water for one day.

***In vitro* ibuprofen release.**

Ibuprofen release via hydrolytic degradation of nanoparticles was evaluated *in vitro* in phosphate buffered saline (PBS, pH = 7.4 or 5.0), as previous work by Stebbins,[35] and Panah[45]. Briefly, 2 mL of blank nanoparticles solution were sealed into dialysis bag (MWCO: 3500) against 30 mL of PBS with different pH, and incubated at 37

Journal of Materials Chemistry B Accepted Manuscript

Please do not adjust margins

View Article Online
DOI: 10.1039/C7TB01288H

Published on 25 July 2017. Downloaded by University of Windsor on 25/07/2017 13:36:54.

°C. At predetermined time intervals, 1 mL of medium was collected and 1 mL of fresh PBS was replaced. The ibuprofen concentration in different samples was calculated by UV-Vis spectra. The amount of ibuprofen was calculated according to a calibration graph. The maximum absorbance wavelength (λ_{max}) of UV-Vis spectra was set to 265 nm. Three groups of replicate measurements were carried out for each time point.

Drug loading and *in vitro* DOX release.

DOX/NPs were prepared as previous studies.[46] Briefly, 3 mg of DOX·HCl and 10 mg of MPEG-PHEI were dissolved in 3 mL DMSO, and 200 μL of TEA was added. 100 μL of this solution was added to 400 μL of Milli-Q water in drop wise. The mixture was stirred at room temperature for 2 hours, and dialyzed by a dialysis bag (MWCO: 3500) against Milli-Q water for one day. The scan speed was 240 nm/min. DOX/NPs were lyophilized to give red powder. The amount of DOX was calculated according to a calibration graph. The λex/em of fluorescence-emission spectra was set to 495/593 nm and the excitation bandwidth was 5.0 nm. Drug loading content (DLC) and loading efficiency (DLE) of DOX was calculated by the following formula:

$$\mathrm{DLC}(\%) = \frac{\text{Weight of loaded DOX}}{\text{Weight of polymer}} \times 100\%$$

$$\mathrm{DLE}(\%) = \frac{\text{Weight of loaded DOX}}{\text{Weight of feeding DOX}} \times 100\%$$

DOX released by polymer hydrolytic degradation was evaluated in PBS (pH = 7.4 or 5.0). 2 mL of DOX/NPs solution were sealed into dialysis bag (MWCO: 3500) against 30 mL of PBS with different pH, and incubated at 37 °C in dark. At predetermined time points, 1 mL of the released medium was withdrawn for fluorescence analysis and 1 mL of PBS was refreshed. The DOX concentration in different samples was calculated by fluorescence-emission spectra as the same way in drug loading section. Three groups of replicate measurements were carried out for each time point.

Cell culture.

B16 murine melanoma cells were purchased from the Cell Bank of the Shanghai Institute of Biochemistry and Cell Biology, Chinese Academy of Sciences (Shanghai, China). The cells were cultured in DMEM with 10% of heat-inactivated FBS. The B16 cells were cultured at 37 °C under a humidified atmosphere of 5% CO_2.

***In vitro* cytotoxicity study.**

The cytotoxic behaviors of blank nanoparticles and DOX/NPs were evaluated using the MTT assay. Cells were seeded into 96-well culture plates at a density of 5000 cells/well, and incubated overnight. Then the culture media were replaced. B16 cells were incubated in media containing MPEG-PHEI or ibuprofen with gradient concentrations of ibuprofen from 0.1 to 1.5 mM (20.6 mg/L to 309.4 mg/L) and media containing DOX/NPs with gradient concentrations of DOX ranging from 0.01 to 5.0 μg/mL, respectively. After that all cell were incubated for 24 h. At the end of the incubation, 100 μL of MTT (5 mg/mL in DMEM) was added to each well and further incubated for 4 h at 37 °C. The medium was removed and added 100 μL of DMSO into each well. The plate was shacked for 10 min at room temperature in dark. The optical density (OD) was then recorded with a SpectraMax M5 microplate reader (Molecular Devices, LLC, Sunnyvale, CA, USA) at 492 nm. Cytotoxicity was expressed as percentage relative to the unexposed control group. Control values were set at 0% cytotoxicity.

***In vitro* cellular uptake.**

B16 cells were seeded on flame-dried coverslips placed in 6-well culture plates at a density of 1×10^5 cells/well. Following incubation overnight, the culture media was refreshed, the cells were cultured with media containing DOX/NPs (containing 10 mg/L of DOX) for 2, 4 and 6 h, as well as DOX·HCl (containing 10 mg/L of DOX) for 2 h. The cells were washed with PBS (pH 7.4) for three times. Then Hoechst 33258 (Biyuntian Biotechnology Co., Shanghai, China) staining was performed (37 °C, 10 min). After staining, cells were washed with PBS twice and the uptake was examined by confocal laser scanning microscope (CLSM, Imager Z2, Zeiss, Oberkochen, Germany).

Wound healing assay.

B16 cells were seeded into 6-well culture plates at a density of 5×10^5 cells/well, and then incubated to grow a cell monolayer. The cell monolayer was scratched with a sterile plastic pipette tip (10 μL) and washed three times with PBS. Scratched B16 cells were exposed to ibuprofen (46.9 mg/L), or MPEG-PHEI (100 mg/L) for 24 h. The cell migration to the wound area was photographed and open wound area was analyzed by ImageJ (Java 1.6.0_24, National Institutes of Health, Bethesda, MD, USA). The rate of migration was measured by quantifying the open wound area before and after treatment.[47]

Western blot analysis.

B16 cells were seeded into each well of 6-well culture plates at a density of 1×10^6 cells/well, and then incubated overnight. B16 cells were treated with ibuprofen (46.9 mg/L) or MPEG-PHEI (100 mg/L) for 24 h and then harvested by cell lysate (with 1 mM of protease inhibitor). Extracts were centrifuged at 12000 g for 10 min at 4 °C, and the supernatants were collected, 100 °C water bath heated for 5 min and stored at –80 °C. The protein concentrations were measured using the BCA protein assay kit (Biyuntian Biotechnology, Co., Shanghai, China).

20 μg protein were separated by sodium dodecyl sulfate–polyacrylamide gel electrophoresis (SDS–PAGE) on 10% (w/v) gels, and then transferred to polyvinylidene difluoride (PVDF) membranes (EMD Millipore, Billerica, MA, USA). Membranes were blocked at room temperature for 1 h by blocking buffer (5% skim milk in TBST, w/v). The membranes were then probed with primary antibodies for COX-2 or GAPDH overnight at 4 °C. After washing with TBST (3×5 min), membranes were incubated with a horseradish peroxidase-conjugated goat anti-mouse and goat anti-rabbit IgG secondary antibodies at room temperature for 1 h. The reactive bands were

Journal of Materials Chemistry B Accepted Manuscript

This journal is © The Royal Society of Chemistry 20xx

View Article Online
DOI: 10.1039/C7TB01288H

Published on 25 July 2017. Downloaded by University of Windsor on 25/07/2017 13:36:54.

detected using Immobilon Western Chemiluminescent HRP Substrate (EMD Millipore) to enhance chemiluminescence.

Animals.

Male BALB/c mice (four weeks old, 18-22 g), and housed in a temperature and illumination regulated environment (25±2 °C, 12 h light/dark cycle). Mice were fed with standard food and water. Animal experimental protocol was approved by Ethics Committee of West China Hospital of Sichuan University.

***In vivo* antitumor assay.**

To investigate the *in vivo* antitumor growth efficiency of DOX·HCl and DOX/NPs, a subcutaneous B16 melanoma tumor models was established. Male BALB/c mice were subcutaneously injected with 1×10^6 B16 cells in 0.1 mL of medium. The mice were then reared for a week when tumor volume reached 100~150 mm^3. Before treatment and the mice were randomly divided into different treatment groups. Mice were given DOX·HCl or DOX/NPs intravenously via the tail vein at a dose of 10 mg DOX equiv./kg., or 46.9 mg ibuprofen equive./kg. every 3-4 days, physiological saline was administrated to another group as control. In the meantime the body weight and the tumor volume of mice were measured. Tumor sizes were measured with a digital caliper, and tumor volumes were calculated by the formula $0.5\times ab^2$, in which **a** is the long tumor diameter and **b** is the short one (mm). Relative tumor volume (RTV) was V/V_0 (V_0 is the initial tumor volume). At the end of the treatment (14 days), mice were sacrificed.

***In vivo* lung metastasis assay.**

To investigate the *in vivo* anti-metastasis efficiency of DOX/NPs, a lung metastasis models was employed. Male BALB/c mice were injected with 1×10^6 B16 cells in 0.1 mL of PBS via tail vein. The mice were randomly assigned to several groups. One hour after injection, the mice were intravenously administered drugs at a dose of 10 mg DOX equiv./kg., or 46.9 mg ibuprofen equive./kg, control group was treated with physiological saline. Then mice were treated in every 3–4 days. Other six mice without injection were raised as normal group. At the end of the treatment (14 days), mice were sacrificed.

Histology and immunohistochemistry.

The heart and tumor tissue of mice with xenograft melanoma tumor, and lung tissue of lung metastasis mice were collected after the mice were sacrificed. The dissected organs and tumors were fixed in 4% paraformaldehyde and processed into paraffin wax, sectioned at 5 μm. Tissue sections were stained with hematoxylin & eosin (H&E). For immunohistochemistry (IH), fixed and embedded tumor and lung tissue specimens were cut into 5 μm sections, and mounted on poly-lysine-coated slides. Tris-EDTA buffer (pH 9.0) was employed for antigen retrieval. To inactivate endogenous peroxides, sections were treated in 3% hydrogen peroxide for 20 min. Sections were blocked with normal goat or mouse serum in PBS at 37 °C for 30 min, and incubated with primary antibodies for COX-2 or Caspase-3 overnight at 4 °C. The horseradish peroxidase-labeled secondary antibody was applied at 37 °C for 30 min. Diaminobenidine (DAB) was adopted as chromogenic substrate. Slides were also counterstained with haematoxylin. Negative controls were treated as previously described, but primary antibodies were replaced by PBS. All tissue samples were examined under microscope to observe histopathological evidence of treatment efficiency.

Statistical analysis.

All data were reported as the mean ± standard deviation (SD). Statistical analysis was performed using SPSS software package Version 19.0 for Windows (SPSS, Inc., Armonk, NY, USA). Statistical significance was analyzed using unpaired, two-tailed Student's t-test. The significance threshold was $P<0.05$.

Results and discussion

Polymers synthesis and characterization.

Firstly, ibuprofen was linked to HEMA with ester bond, as shown in Scheme 2, giving a founctional monomer which could be used for further polymerization. To achieve pH-sensitive property, benzoic-imine bond was introduced into the PEG coating. Since its π–π conjugation, benzoic-imine bond is steady in basic or neutral surrounding, but it will hydrolyze in acidic environment. Finally, the targeted polymer was polymerized via ATRP method using PEG-CBA-Br as the macroinitiator. With the ibuprofen releasing via ester bond hydrolytsis, and the pH–sensitive property of benzoic-imine bond, the target delivery and release of both ibuprofen and DOX into cancer cells could be accomplished.

^{1}H NMR was employed to confirm the chemical structures of precursors and MPEG-PHEI. ^{1}H NMR spectrum also verified polymer achieved a relatively high drug loading (46.9 wt % of ibuprofen) as we expected.[35] GPC results showed the low molecular weight distribution (PDI less than 1.2, shown in Fig. S2) of MPEG-PHEI.

Characterizations of blank nanoparticles and DOX/NPs.

To investigate the self-assembly behavior of amphiphilic MPEG-PHEI, pyrene was used as a probe for fluorescence measurement. The absorption band shifts from 334 nm to 338 nm as the increasing concentration, and the fluorescence intensity ratio of 338 nm and 334 nm (I_{338}/I_{334}) was calculated. The function of I_{338}/I_{334} and the logarithm concentrations (LgC) is shown in Figure 2A. The concentration, 2.5×10^{-3} mg/mL, at intersection of two tangent lines was the CMC value, indicating that MPEG-PHEI showed decent tendency to self-assemble in aqueous environment.

Then nanoparticles were prepared and studied by DLS and TEM. As shown in Figure 2C, the particle diameters were measured by DLS, and average diameter was around 190 nm. The morphology of nanoparticles was observed by TEM, shown in Figure 2D. The TEM images suggested that the nanoparticles were spherical, and the diameter was less than 200 nm. The sizes determined by TEM and DLS were different, since the TEM image is obtained in a dry state. After loaded with DOX, the diameter of DOX/NPs was measured by the DLS as a comparison shown in Figure S2. The mean size of DOX/NPs was 213.7 nm because the loading of DOX in the

Journal of Materials Chemistry B Accepted Manuscript

Please do not adjust margins

View Article Online
DOI: 10.1039/C7TB01288H

Published on 25 July 2017. Downloaded by University of Windsor on 25/07/2017 13:36:54.

hydrophobic core increased the core diameter. Both diameters of blank nanoparticles and DOX/NPs were amenable to cell internalization.[48, 49]

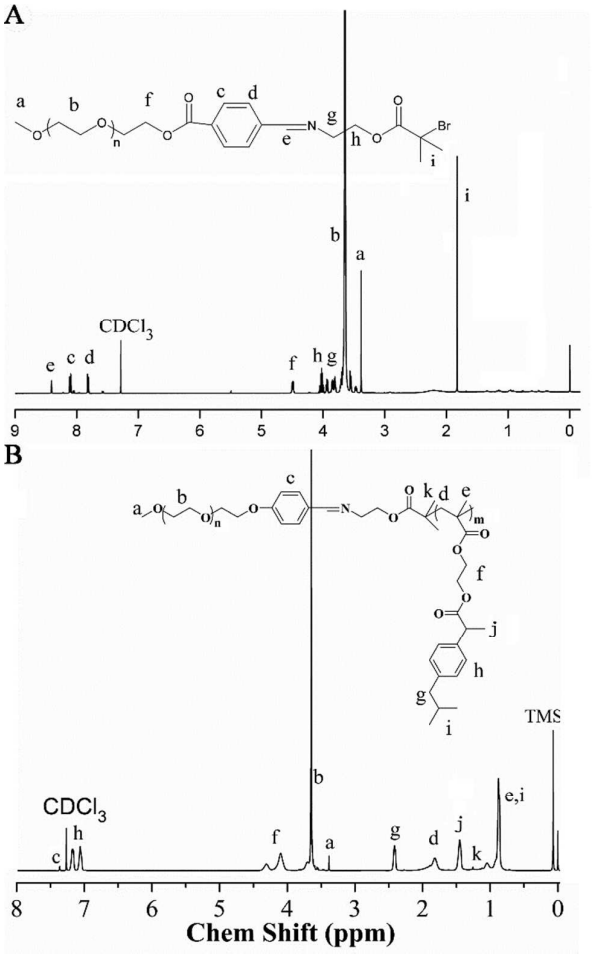

Figure 1 ^{1}H-NMR spectra of PEG-CBA-Br (A) and MPEG-PHEI (B) in $CDCl_3$.

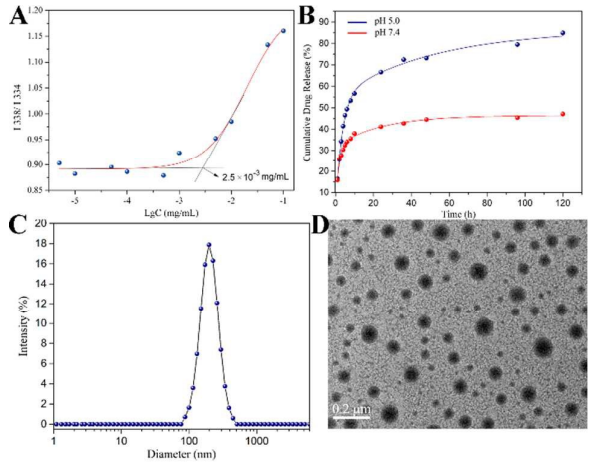

Figure 2 Critical micelles concentration (A) ascertained by the function of excitation intensity ration of pyrene at 338 and 334 nm (I338/I334) vs the polymer concentrations in water. The cumulative DOX release profiles of DOX/NPs (B), in physiological and acidic conditions (37 °C, pH 7.4 and 5.0). Size distribution (C) and morphology characteristics (D) of blank nanoparticles. The scale bar of the TEM is 0.2 μm.

Drug loading and *in vitro* release.

Since DOX was employed as the hydrophobic anticancer drug, DOX loading content was measured by its fluorescence. DOX was loaded in nanoparticles via dialysis, and then the DOX/NPs were lyophilized. According to the equations in Materials and Methods section, the DLC and DLE of nanoparticles were 10.0% and 33.4%. The release behavior of DOX from vehicles was examined at physiological and acidic conditions. The amount of released DOX in media was measured by fluorescence. The DOX releasing was controlled by nanoparticles collapse from cleavable benzoic-imine. Therefore, under weak acidic condition the release rates were relatively higher, and the amount of cumulative released DOX over the same period of time was bigger. As shown in Figure 2B, under physiological conditions, ~35% of DOX was released in first 10 h, however, more than 55% of DOX was released at pH 5.0 under the same conditions. After 120 h of experiment, the release of DOX was 85.0%. These results suggested the acidic condition reinforced the collapse of nanoparticles, and release of DOX rapidly at acidic endosome condition. As for ibuprofen, the release of ibuprofen was investigated by UV-vis spectra. As shown in Figure S4, MPEG-PHEI exhibited a faster ibuprofen release in acidic condition throughout the 14-day experiment. Ibuprofen release is controlled by both nanoparticles collapse and ester bond hydrolysis. Based on previous studies using NSAID-containing nanoparticles, more labile nanoparticles cleave first, followed by ester bond hydrolysis.[34, 50]

***In vitro* cytotoxicity of DOX/NPs.**

Bioactivity and safety are two important factors in order to realize further use for synthetic biomaterials. The *in vitro* cytotoxicity of blank nanoparticles and DOX/NPs was evaluated by MTT assay. Figure 3A showed the cytotoxicity of different concentrations of ibuprofen and blank nanoparticles to B16 cells. After treatment for 24 h, both blank nanoparticles and ibuprofen (concentration of ibuprofen ranging from 0.1 to 1.5 mM) showed no significant growth inhibition effect. Then B16 cells were incubation with DOX and DOX/NPs for 24 h. As show in Figure 3B, the dose-depend cell inhibition for both DOX·HCl and DOX/NPs were observed. DOX/NPs showed a weaker cytotoxicity than DOX·HCl, especially in at low concentration, because of the prolonged release from the nanoparticles and different cellular uptake way of DOX. The results were consistent with the followed cellular uptake results. The IC_{50} of DOX·HCl and DOX/NPs was 0.315 and 0.638 μg/mL respectively.

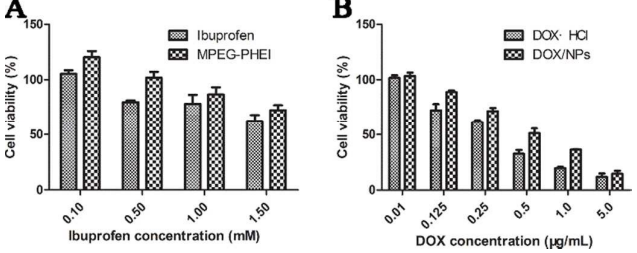

Figure 3 Cytotoxicity of blank nanoparticles and ibuprofen (A), DOX/NPs and DOX·HCl (B) on B16 cells for 24h. Error bars indicate SD (n = 3).

Journal of Materials Chemistry B Accepted Manuscript

This journal is © The Royal Society of Chemistry 20xx

Please do not adjust margins

View Article Online
DOI: 10.1039/C7TB01288H

Published on 25 July 2017. Downloaded by University of Windsor on 25/07/2017 13:36:54.

Cellular uptake of DOX/NPs.

In this work, DOX was employed as the model drug due to its anticancer activity and intrinsic red fluorescence. Since the intracellular fluorescence intensity reflected the DOX amount absorbed by cells, the DOX uptake and location in B16 cells were visualized by CLSM. With an increasing treated time (from 2 h to 6 h), the red fluorescence inside the cells intensifies became stronger visually shown in Figure 4A, B and C. But even in cells treated with the DOX/NPs for 6 h, the red fluorescence intensity was weaker than it in cells treated with DOX·HCl for 2 h. In DOX·HCl treated cells, the red fluorescence mainly overlapped with blue fluorescence in nucleus, shown in Figure 4D. By comparison, the red fluorescence signals from NPs mainly distributed in cytoplasm. It was endocytosis way of nanoparticle internalization that lead to the difference. These results were impressive evidence of DOX/NPs got into the tumor cells via endocytosis and released DOX in cytoplasm.

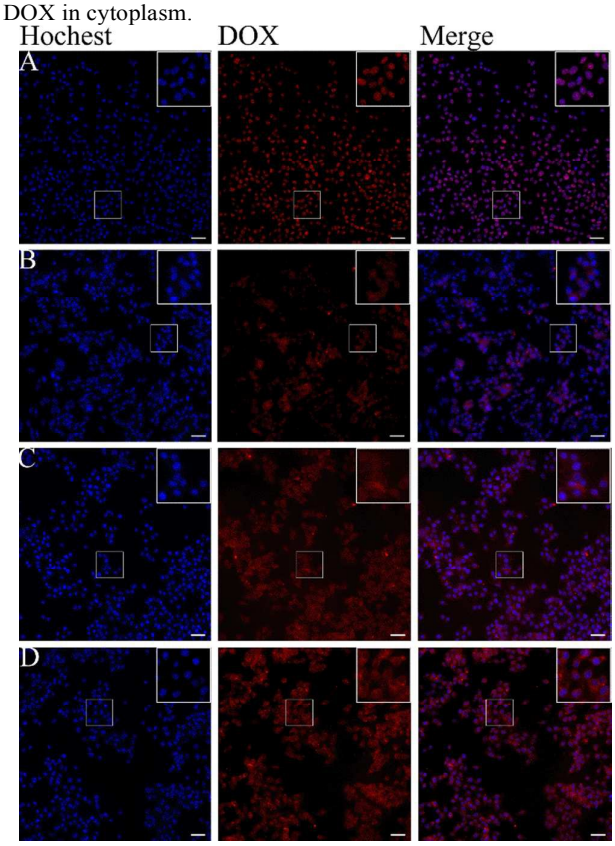

Figure 4 Fluorescence microscopy images of intracellular uptake of DOX (red), treated by DOX·HCl for 2 h (A), DOX/NPs for 2 h (B), 4 h (C), and 6 h (D). Nuclei were labeled with Hoechest (blue). The scale bar is 50 μm.

Inhibition of MPEG-PHEI against COX-2 expression and migration in B16 cells.

The inhibition of MPEG-PHEI against B16 cell migration was tested by the wound healing assay. The effect of MPEG-PHEI treatment on B16 cell migration was shown in Figure 5A, after treatment with MPEG-PHEI for 24 h, cell migration was notably inhibited with the wound area ~80.1% compared to wound area ~40.6%in control group. Moreover, the wound area of MPEG-PHEI treated group was comparable to ibuprofen treated group (wound area ~81.1%). The *in vitro* COX-2 inhibition bioactivity in B16 cells of MPEG-PHEI was studied by Western blot. As shown in Figure 5C, GAPDH was used as an internal reference, and the expression of COX-2 in both ibuprofen and MPEG-PHEI treated groups were significantly down-regulated compared to control group. These results indicated that the MPEG-PHEI could effectively inhibit B16 cell migration and COX expression, suggesting that the ibuprofen in MPEG-PHEI could be released to the free form retaining its activity.

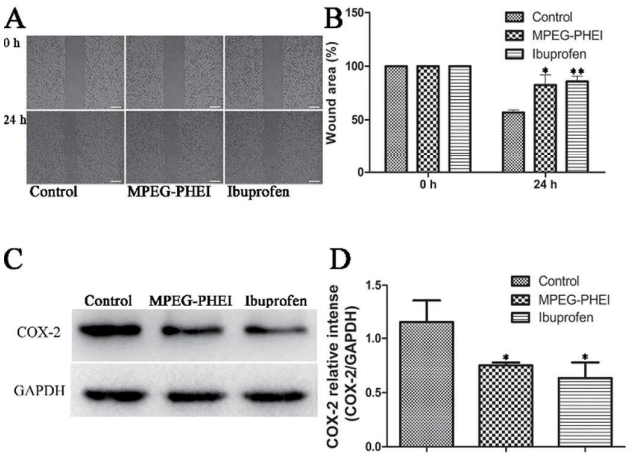

Figure 5 Wound healing assay in B16 cells treated with ibuprofen and MPEG-PHEI for 24 h (A), quantification of wound area in control, ibuprofen and MPEG-PHEI treated B16 cells (B).Western blot (C) and protein expression level of COX-2 in B16 cells (D) treated with MPEG-PHEI and ibuprofen for 24 h, GAPDH was used as internal reference. Error bars indicate SD (n = 3). *P < 0.01, **P < 0.005, treated group versus control group. The scale bar is 50 μm.

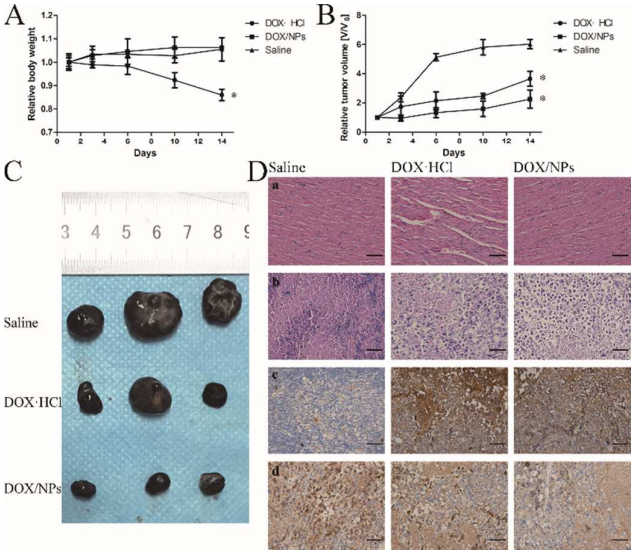

Figure 6 *In vivo* antitumor efficacy of DOX/NPs. (A) Body weights of mice, (B) tumor growth curves, (C) tumor morphologies after the mice were sacrificed, (D) H&E staining of heart sections (a) and tumor sections (b) harvested from each groups, IH staining of Caspase-3 (c) and COX-2 (d) in tumor sections from different groups. Error bars indicate SD (n = 6). *P < 0.01, treated group versus saline group. The scale bar is 500 μm.

***In vivo* antitumor efficacy of DOX/NPs.**

Journal of Materials Chemistry B Accepted Manuscript

Please do not adjust margins

View Article Online
DOI: 10.1039/C7TB01288H

Published on 25 July 2017. Downloaded by University of Windsor on 25/07/2017 13:36:54.

As shown in Figure 6A, DOX/NPs and saline groups showed no obvious changes in body weight, whereas DOX·HCl group exhibited a notably decrease, because of inherent systemic toxicity of DOX·HCl. Compared to control group, both DOX/NPs and DOX·HCl exhibited tumor inhibition efficacy. The RTV for saline, DOX/NPs and DOX·HCl treated group treated group at day 14 was ~6.0, 2.3 and 3.6, respectively. The photo of isolated tumor in figure 6C confirmed DOX/NPs was more effective than DOX·HCl on tumor growth suppression *in vivo*. Furthermore, the histological assay of tumor and heart after treatment were performed using H&E staining or immunohistochemistry. H&E assays of hearts indicated that DOX/NPs caused little damage to heart but widespread apoptosis in tumor. In DOX·HCl group, more significant heart damage was observed.

Immunohistochemistry study in Figure 6D showed that both DOX·HCl and DOX/NPs induced Caspase-3 expression in tumor tissue and DOX/NPs treatment decreased the COX-2 expression in tumor tissue. These finding indicated that DOX/NPs could tumor-targeted kill B16 cells by apoptosis mechanisms as DOX·HCl, with reduced the side effect. These results revealed that DOX/NPs could enhance antitumor efficiency, and relieve weight loss issue of DOX·HCl.

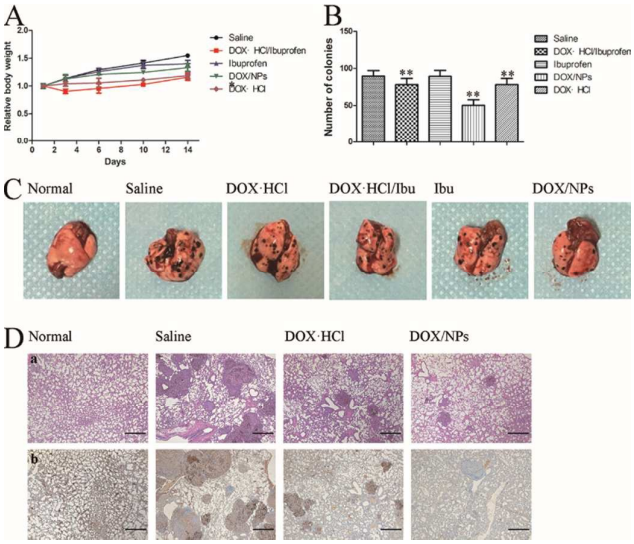

Figure 7 DOX/NPs reduce metastasis of B16 melanoma cells to lung in mice. (A) Body weights of mice, (B) the number of visible lung colonies in lung of each group after treatment, (C) lung morphologies after the mice were sacrificed, (D) H&E staining of lung sections harvested from each groups (a) and IH staining of COX-2 (b) in lung sections from different groups. Error bars indicate SD (n = 6). *P < 0.01, **P < 0.005, treated group versus saline group. The scale bar is 500 μm.

Anti-metastasis efficacy of DOX/NPs.

Taking into consideration the migration inhibition of MPEG-PHEI obtained in cell assays, we investigated the antimetastatic effect of DOX/NPs against B16 cells *in vivo*. After two weeks of treatment, significant reduction of tumor nodules was observed on lungs in DOX/NPs treated animals, but DOX·HCl, ibuprofen, as well as the combination of DOX·HCl and ibuprofen showed weaker antimetastatic efficacy on tumor nodules, as shown in Figure 7B and C. Based on previous researches, DOX/NPs might improve therapeutic effect of DOX·HCl and ibuprofen via enhanced permeation and retention (EPR) effect.[22, 23] H&E staining showed a significant reduction of the tumor mass and lung-infiltrating tumor cells in lungs of DOX/NPs group animals, in Figure 7D a. Moreover, immunohistochemistry study revealed that DOX/NPs treatment markedly reduced COX-2 expression in lung, shown in Figure 7D b These results confirmed the antimetastatic activity in cell study, and indicated that DOX/NPs exert antimetastatic activity *in vivo*.

Conclusions

In this paper, a novel pH responsive amphiphilic and biodegradable block copolymer, MPEG-PHEI based on PEG and ibuprofen was synthesized successfully. MPEG-PHEI could self-assemble into nanoparticles to form a classic "core–shell" structure in aqueous solution with an appropriate mean particle diameter around 200 nm. Moreover, DOX/NPs had proper drug loading content of DOX and ibuprofen, as well as pH sensitivity. DOX/NPs could internalize into B16 cells through endocytosis and kill B16 cells. MPEG-PHEI could release ibuprofen through hydrolysis, and the released ibuprofen retained activity to inhibit the COX-2 expression and migration of B16 cells. Furthermore, DOX/NPs exerted compared anti-tumor activity to DOX·HCl, and inhibited melanoma metastasis to lung in mice. This research provided a promising drug delivery system combining NASIDs with antineoplastic drugs, which could be a potential alternative in chemotherapy for cancer.

Acknowledgements

This study was partly supported by the China National '12.5' Foundation (Grant No. 2011BAJ07B04), and National Natural Science Foundation of China (Grant No. 81673710 and 51503130).

Notes and references

1 D. L. Cummins, J. M. Cummins, H. Pantle, M. A. Silverman, A. L. Leonard and A. Chanmugam, *Clinics in Dermatology*, 2006, **81**, 500-507.
2 P. S. Steeg, *Nature Medicine*, 2006, **12**, 895-904.
3 P. Mehlen and A. Puisieux, *Nature reviews. Cancer*, 2006, **6**, 449-458.
4 A. Ortega, *Trends in Pharmacological Sciences*, 2003, **24**, 151.
5 I. J. Fidler, *Seminars in Cancer Biology*, 2002, **12**, 89-96.
6 P. S. Steeg and D. Theodorescu, *Nature Clinical Practice Oncology*, 2008, **5**, 206.
7 O. A. Martin, R. L. Anderson, K. Narayan and M. R. MacManus, *Nat. Rev. Clin. Oncol.*, 2017, **14**, 32-44.
8 D. Oka, K. Nishimura, M. Shiba, Y. Nakai, Y. Arai, M. Nakayama, H. Takayama, H. Inoue, A. Okuyama and N. Nonomura, *International Journal of Cancer*, 2007, **120**, 2576-2581.
9 D. Z. Wang and R. N. Dubois, *Nat. Rev. Cancer*, 2010, **10**, 181-193.
10 T. T. Fang, J. Y. Hou, M. Y. He, L. Y. Wang, M. H. Zheng, X. D. Wang and J. L. Xia, *Cell Biol. Toxicol.*, 2016, **32**, 499-511.
11 H. Takahashi, A. H. Li, D. W. Dawson, O. J. Hines, H. A. Reber and G. Eibl, *Pancreas*, 2011, **40**, 453-459.

Journal of Materials Chemistry B Accepted Manuscript

This journal is © The Royal Society of Chemistry 20xx

Please do not adjust margins

View Article Online
DOI: 10.1039/C7TB01288H

12 C. Tabolacci, A. Lentini, B. Provenzano, A. Gismondi, S. Rossi and S. Beninati, *Melanoma Research*, 2010, **20**, 273-279.
13 F. E. Silverstein, G. Faich, J. L. Goldstein, L. S. Simon, T. Pincus, A. Whelton, R. Makuch, G. Eisen, N. M. Agarwal, W. F. Stenson, A. M. Burr, W. W. Zhao, J. D. Kent, J. B. Lefkowith, K. M. Verburg and G. S. Geis, *Jama-Journal of the American Medical Association*, 2000, **284**, 1247-1255.
14 J. R. Vane, Y. S. Bakhle and R. M. Botting, *Annual Review of Pharmacology and Toxicology*, 1998, **38**, 97-120.
15 T. Li, J. Zhong, X. Dong, P. Xiu, F. Wang, H. Wei, X. Wang, Z. Xu, F. Liu, X. Sun and J. Li, *Oncology Reports*, 2016, **35**, 3614-3622.
16 K. M. Kim, A. R. Im, S. H. Kim, J. W. Hyun and S. Chae, *Cancer Science*, 2016, **107**, 181-188.
17 A. Zlotnik, *Involvement of Chemokine Receptors in Organ-Specific Metastasis*, Karger Publishers, 2006.
18 R. K. Pathak, S. Marrache, J. H. Choi, T. B. Berding, Prof., #x and D. S. Dhar, *Angewandte Chemie*, 2014, **53**, 1963-1967.
19 R. Calaluce, D. L. Earnest, D. Heddens, J. G. Einspahr, D. Roe, C. L. Bogert, J. R. Marshall and D. S. Alberts, *Cancer epidemiology, biomarkers & prevention : a publication of the American Association for Cancer Research, cosponsored by the American Society of Preventive Oncology*, 2000, **9**, 1287.
20 R. E. Harris, R. T. Chlebowski, R. D. Jackson, D. J. Frid, J. L. Ascenseo, G. Anderson, A. Loar, R. J. Rodabough, E. White and A. Mctiernan, *Cancer Res.*, 2003, **63**, 6096-6101.
21 M. Paul, K. Sarkar, J. Deb and P. Dastidar, *Chemistry-a European Journal*, 2017, **23**, 5736-5747.
22 H. Maeda, J. Wu, T. Sawa, Y. Matsumura and K. Hori, *J. Control. Release*, 2000, **65**, 271-284.
23 J. Fang, H. Nakamura and H. Maeda, *Adv. Drug Deliv. Rev.*, 2011, **63**, 136-151.
24 H. Maeda, *Bioconjugate Chemistry*, 2010, **21**, 797-802.
25 A. M. Butt, M. C. I. M. Amin, H. Katas, N. A. A. Murad, R. Jamal and P. Kesharwani, *Molecular Pharmaceutics*, 2016, **13**, 4179-4190.
26 F. Li, W.-l. Chen, B.-g. You, Y. Liu, S.-d. Yang, Z.-q. Yuan, W.-j. Zhu, J.-z. Li, C.-x. Qu, Y.-j. Zhou, X.-f. Zhou, C. Liu and X.-n. Zhang, *Acs Applied Materials & Interfaces*, 2016, **8**, 32146-32158.
27 X. Wang, H. Hu, W. Wang, K. I. Lee, C. Gao, L. He, Y. Wang, C. Lai, B. Fei and J. H. Xin, *Colloids and Surfaces B-Biointerfaces*, 2016, **143**, 342-351.
28 K. Tian, X. Jia, X. B. Zhao and P. Liu, *Molecular Pharmaceutics*, 2016, **13**, 2683-2690.
29 C. Zuo, X. Y. Dai, S. J. Zhao, X. N. Liu, S. L. Ding, L. W. Ma, M. Z. Liu and H. Wei, *ACS Macro Lett.*, 2016, **5**, 873-878.
30 Y. Huang, Z. H. Tang, X. F. Zhang, H. Y. Yu, H. Sun, X. Pang and X. S. Chen, *Biomacromolecules*, 2013, **14**, 2023-2032.
31 D. Neri and C. T. Supuran, *Nat. Rev. Drug Discov.*, 2011, **10**, 767-777.
32 E. S. Lee, Z. G. Gao and Y. H. Bae, *J. Control. Release*, 2008, **132**, 164-170.
33 R. Liu, A. H. Colby, D. Gilmore, M. Schulz, J. L. Zeng, R. F. Padera, O. Shirihai, M. W. Grinstaff and Y. L. Colson, *Biomaterials*, 2016, **102**, 175-186.
34 S. Ganta, H. Devalapally, A. Shahiwala and M. Amiji, *J. Control. Release*, 2008, **126**, 187-204.
35 N. D. Stebbins, W. L. Yu and K. E. Uhrich, *Biomacromolecules*, 2015, **16**, 3632-3639.
36 U. Hasegawa, A. J. van der Vlies, C. Wandrey and J. A. Hubbell, *Biomacromolecules*, 2013, **14**, 3314-3320.
37 S. Lee, X. M. Tong and F. Yang, *Biomater. Sci.*, 2016, **4**, 405-411.
38 Y. Li, M. Kroger and W. K. Liu, *Biomaterials*, 2014, **35**, 8467-8478.
39 R. L. Siegel, K. D. Miller and A. Jemal, *CA-Cancer J. Clin.*, 2017, **67**, 7-30.
40 R. E. Kast, *Med. Oncol.*, 2007, **24**, 1-6.
41 C. Cahlin, J. Gelin, D. Delbro, C. Lonnroth, C. Doi and K. Lundholm, *Cancer Res.*, 2000, **60**, 1742-1749.
42 C. Denkert, M. Kobel, S. Berger, A. Siegert, A. Leclere, U. Trefzer and S. Hauptmann, *Cancer Res.*, 2001, **61**, 303-308.
43 N. Song, M. Ding, Z. Pan, J. Li, L. Zhou, H. Tan and Q. Fu, *Biomacromolecules*, 2013, **14**, 4407-4419.
44 H. L. Guan, Z. G. Xie, P. B. Zhang, C. Deng, X. S. Chen and X. B. Jing, *Biomacromolecules*, 2005, **6**, 1954-1960.
45 N. G. Panah, P. Alizadeh, B. E. Yekta and N. Motakef-Kazemi, *Ceram. Int.*, 2016, **42**, 10935-10942.
46 Y. Zhang, J. L. He, D. L. Cao, M. Z. Zhang and P. H. Ni, *Polym. Chem.*, 2014, **5**, 5124-5138.
47 X. Yang, Y. Xu, T. Wang, D. Shu, P. Guo, K. Miskimins and S. Y. Qian, *Redox Biology*, 2017, **11**, 653-662.
48 M. Ansar, D. Serrano, I. Papademetriou, T. K. Bhowmick and S. Muro, *ACS Nano*, 2013, **7**, 10597-10611.
49 I. Canton and G. Battaglia, *Chem. Soc. Rev.*, 2012, **41**, 2718-2739.
50 D. Sutton, N. Nasongkla, E. Blanco and J. Gao, *Pharmaceutical Research*, 2007, **24**, 1029-1046.

Published on 25 July 2017. Downloaded by University of Windsor on 25/07/2017 13:36:54.

Journal of Materials Chemistry B Accepted Manuscript

Please do not adjust margins